Available online at www.sciencedirect.com
SCIENCE DIRECT®
European Journal of Pharmaceutics and Biopharmaceutics 58 (2004) 25–35
European Journal of Pharmaceutics and Biopharmaceutics
www.elsevier.com/locate/ejpb

Research paper

Physicochemical characterisation of cationic polybutylcyanoacrylat-nanoparticles by fluorescence correlation spectroscopy

Jörg Weyermann[a,1], Dirk Lochmann[a,1], Christiane Georgens[a], Isam Rais[b], Jörg Kreuter[a], Michael Karas[b], Markus Wolkenhauer[c], Andreas Zimmer[d,*]

[a]*Institute for Pharmaceutical Technology, Johann Wolfgang Goethe-University, Frankfurt am Main, Germany*
[b]*Institute for Pharmaceutical Chemistry, Johann Wolfgang Goethe-University, Frankfurt am Main, Germany*
[c]*Max-Planck-Institute of Polymer Research, Mainz, Germany*
[d]*Institute of Pharmaceutical Chemistry and Pharmaceutical Technology, Karl-Franzens-University, Graz, Austria*

Received 20 October 2003; accepted in revised form 2 February 2004

Available online 2 April 2004

Abstract

The aim of this study was to compare different physical and chemical methods with fluorescence correlation spectroscopy (FCS) in order to characterise cationic acrylate nanoparticles (NP), which can deliver oligonucleotides (ON) into mammalian cells. These positively charged nanoparticles were prepared from diethylaminoethyl dextran (DEAE-dextran) and poly(*n*-butyl-2-cyanoacrylate) (PBCA). NP consists of PBCA oligochains with an average size of PBCA 9 mer and were formed by entrapping DEAE-dextran and dextran 70,000 in high amounts into the particle matrix. The oligochain length of PBCA was investigated by mass-spectroscopy (MALDI TOF). The molecular weight of a particle with $d = 108$ nm was estimated to be approximately 3.6×10^8 Da. The mean size of the nanoparticles were in a range of $d_h = 130-140$ nm, as determined independently by FCS and dynamic light scattering. Atomic force microscopy and scanning electron microscopy images confirm this size range. Furthermore, the particle mass of the PBCA-NP was estimated by FCS measurements. For this approach two new methods for fluorescence labelling of cationic particles were developed. Fluorescent labelled dextran 70,000 was entrapped into the particle matrix; in addition, the derivatisation of hydroxyl groups of the NP was achieved with 5-([4,6-dichlorotriazin-2-yl]amino) fluorescein (DTAF). ON can be localised in a complex with the NP by dual-colour fluorescence cross correlation spectroscopy measurements. The zetapotential of the unloaded NP was positively charged with about +39 mV and decreased down to −40 mV on addition of excess ON. After centrifugation quantification of the ON loading onto the particles by strong anion exchange high performance liquid chromatography (SAX HPLC) and FCS showed that approximately 20 μg ON per 100 μg NP was adsorbed. The FCS measurements of the ON adsorption in situ was found to be much higher with approximately 95 μg ON per 100 μg NP.

Keywords: Fluorescence correlation spectroscopy; Nanoparticles; Acrylate; DEAE-dextran; Oligonucleotides; Poly(*n*-butyl-2-cyanoacrylate); Drug delivery system; DNA; Phosphorothioate

1. Introduction

Nanoparticles (NP) are solid colloidal drug carriers ranging from 10 to 1000 nm in diameter. These NP consist of macromolecules in which a drug is entrapped, encapsulated or adsorbed onto the surface. Those of nanoparticles or nanospheres as a drug delivery system has been described previously by Kreuter [1].

DNA as a drug is a new challenge in pharmaceutics since a few years. Antisense-oligonucleotides are short single stranded DNA or RNA molecules (15–25 nucleotides) [2]. These oligonucleotides (ON) are effective blocking agents of protein expression (e.g. through translation arrest) with a high sequence specificity as described first in 1978 [3,4]. Unfortunately, oligonucleotide drugs are considered to be degraded by nucleases [5] and they exhibit only a weak permeation through biological cell membranes resulting in a poor bioavailability [6]. Therefore, a strong need exists for

* Corresponding author. Institute of Pharmaceutical Chemistry and Pharmaceutical Technology, Karl-Franzens-University Graz, Schubertstraße 6, 8010 Graz, Austria. Tel.: +43-316-380-8881; fax: +43-316-380-9100.
E-mail address: andreas.zimmer@uni-graz.at (A. Zimmer).
[1] Dirk Lochmann and Jörg Weyermann contributed equally to this work.

0939-6411/$ - see front matter © 2004 Elsevier B.V. All rights reserved.
doi:10.1016/j.ejpb.2004.02.011

delivery systems which protect the antisense drugs from enzymatic digestion and which provide an enhanced transfection to the cytoplasm of the target cells [7].

One well described delivery system for ON are cationic nanoparticles which consist of acrylate. Several different acrylate materials have been used [8–12]. Poly(*i*-butyl-2-cyanoacrylate) nanoparticles are currently in preclinical trials as carriers for doxorubicin. The acrylate monomer poly(*n*-butyl-2-cyanoacrylate) (PBCA) was used to prepare cationic NP, which were shown to deliver plasmids into cells [13]. We applied this monomer in combination with diethylaminoethyl dextran (DEAE-dextran) which was entrapped into the particle matrix, similar to the formulations with poly(*n*-hexyl-2-cyanoacrylate) as described before by Zobel [14].

For loading of NP, oligonucleotides were adsorbed onto the particle surface, using ion pair interaction of the negatively charged oligonucleotide backbone and the bounded DEAE-dextran.

The aim of this work was to characterise cationised poly(*n*-butyl-cyano-2-acrylate) nanoparticles (PBCA-NP) and their interaction with oligonucleotides using the fluorescence correlation spectroscopy (FCS) technique, in comparison to generally accepted methods of particle size measurements, zetapotential measurements and further analytical methods. The theoretical concept of FCS was already generated in the 1970s [15], the insertion of a confocal microscope in the 1990s improved this technique to a great extent. FCS is now probably the most famous single-molecule-fluorescence-detection method [16]. It discerns fluctuations in fluorescence intensity of single fluophores in highly diluted solutions which can be correlated to the diffusion time of these molecules. Thus FCS provides the opportunity to receive information on diffusion properties, molecular weights and molecular interactions.

To confirm the data from FCS, the particle size was measured by a dynamic light scattering method (DLS) based on photon correlation spectroscopy [17,18]. The shape was determined by atomic force microscopy (AFM) and scanning electron microscopy (SEM). Furthermore, the focus of this work was to correlate between oligonucleotide loading capacity of the particles by HPLC analysis under strong anion exchange conditions (SAX HPLC) [19] and new in situ measurements by FCS. Also the influence of the ON-loading on the surface charge was determined and compared to the FCS measurements [20–22]. Additionally, we concentrated on investigations to identify the composition of NP and developed two new preparation methods for fluorescence labelled cationic acrylate-NP.

2. Material and methods

2.1. Materials

Fully thioated oligonucleotides (ON) used in this study were synthesised by MWG Biotech (Ebersberg, Germany). They consisted of the following sequence: 5′-CTA GGA TCT ACT GGC TCC AT-3′ (MW 6068 Da). We also purchased this sequence with a fluorescence label of tetraethylrhodamine (Rhod B) respectively Cy™5 on the 5′-end. All ON were 'high purity salt free' (HPSF®-quality) and analysed by mass spectroscopy (MALDI-TOF MS documentation). The *n*-butyl-2-cyanoacrylate monomer was purchased from Sichel Werke (Hannover, Germany). Sodium perchlorate was obtained from Merck (Darmstadt, Germany). Cy™5 was obtained from Amersham Pharmacia Biotech (Freiburg, Germany). Rhod B-dextran with a molecular weight of 70,000 Da was purchased from Molecular Probes (MoBiTec, Göttingen). Unlabelled dextran (dextran 70,000) and fluorescein-dextran (FITC-dextran) each with a molecular weight of 70,000 Da, diethylaminoethyl dextran (DEAE-dextran) with a molecular weight of 500,000 Da, fluorescein (FITC), Rhod B and all other chemicals were of the highest available purity and were obtained from Sigma (Taufkirchen, Germany). Water was purified with a Milli-Q Plus system obtained from Millipore (Schwalbach, Germany).

2.2. Methods

2.2.1. Particle preparation

Poly(*n*-butyl-2-cyanoacrylate) nanoparticles are produced by an aqueous dispersion polymerisation technique involving anionic emulsion polymerisation of butylcyanoacrylate in the presence of a stabilising agent. In our case we used dextran 70,000 as already described before [23,24]. To change the surface charge of the resulting NP, DEAE-dextran was added prior to polymerisation, based on a method introduced by Zobel [14] for poly(*n*-hexyl-2-cyanoacrylate) nanoparticles.

2.2.1.1. Method A (non-fluorescent particles: NP-A). Poly(*n*-butyl-2-cyanoacrylate) nanoparticles were prepared by an aqueous dispersion polymerisation process from *n*-butyl-2-cyanoacralyte monomers (Table 1). Amounts of 250 mg (1% w/v) of either dextran 70,000/DEAE-dextran mixture (ratio 60:40) were dissolved in 25 ml of 0.01 N hydrochloric acid (HCl) solution while stirring on a magnetic stirring plate at 500 rpm (Variomag-Multipoint, Dr Hoiss, Munich, Germany). After this, 250 μl of *n*-butyl-2-cyanoacrylate were carefully added, and stirring was continued for 4 h at 20 °C to assure polymerisation of the monomer. Afterwards the polymerisation was stopped by neutralisation of the solution with 1 N sodium hydroxide. Larger polymer aggregates were separated from the nanoparticles by filtration through 0.45 μm filtration units. The suspension were stable for several weeks at 4 °C.

2.2.1.2. Method B (fluorescent particles by entrapping Rhod B-dextran/FITC-dextran: NP-B). The preparation followed method A, except that 10% of the dextran 70,000 was

Table 1
Ingredients of the particle-preparation

Method	SICO MET 6000 (PBCA) (mg)	Dextran 70,000 (mg)	DEAE-dextran (mg)	Rhod B-/FITC-dextran (mg)	DTAF
A	250	150	100	–	–
B	250	135	100	15	–
C	250	150	100	–	+

replaced by Rhod B-labelled dextran or FITC-labelled dextran with the same molecular weight. These batches contained 250 mg PBCA, 135 mg dextran 70,000, 15 mg Rod B-dextran/FITC-dextran and 100 mg DEAE-dextran with a molecular weight of 500,000 Da.

2.2.1.3. Method C (fluorescent particles by derivatisation with DTAF: NP-C). After polymerisation, neutralisation and filtration according to method A, the resulting colloidal stock solution was purified by dialysis through a semi-permeable membrane with an exclusion size of 1,000,000 Da (Spectra/Por CE Membrane MWCO 1,000,000 from Spectrum Laboratories Inc.) against purified water for 48 h. Afterwards we added 1 mg of particles (equivalent to 71 μl dialysed stock solution) to 5 ml 5-([4,6-dichlorotriazin-2-yl]amino) fluorescein (DTAF) solution (0.2 mg/ml DTAF in 0.1 M borate buffer; pH 9). After 12 h at room temperature, under constant stirring, 1 N HCl was added until the pH reached 7. In order to remove all free DTAF, the solution was dialysed again according to the procedure described above.

2.2.2. Atomic force microscopy

To obtain information about the substructure and topography of the dried nanoparticles, AFM measurements were carried out. The samples were prepared by lyophilisation of the colloidal particle suspension on mica. Commercially available atomic force microscope (Multimode, NanoScope 3, Veeco Instruments, Santa Barbara, CA) was used. The microscope was calibrated using a standard grating with a known lattice spacing. Rectangular silicon cantilevers (Olympus, Japan; 160 μm long, 50 μm wide, 4.6 μm thick, aluminium coated on back) with an integrated tip, a nominal spring constant of 42 N/m, and a resonance frequency of 200–400 kHz were used for the measurements. All measurements were performed in tapping mode. This special mode enables AFM of soft materials. In contact mode the probe (tip) at the end of the cantilever is in permanent contact with the surface, whereas in tapping mode the interaction time of the tip with the surface is very short. Therefore, damages and scratches can be avoided. In this mode the cantilever oscillates near its free resonance frequency. Due to interaction forces (e.g. van der Waals) near the surface the resonance frequency is shifted leading to large amplitudes. The tip hits the surface and is withdrawn immediately, so contact time and scratching is minimized while the probe is tapping on the surface.

2.2.3. Scanning electron microscopy

100 μl of the particle preparation were freeze dried on a polished aluminium surface. After the drying process the sample was sputtered with gold for 30 s under argon atmosphere (Agar sputter coater). Afterwards SEM was performed with a S-4500 Hitachi field emission electron microscope (Krefeld, Germany) with the upper detector at 25 kV. The magnification was approximately 80,000. The sample plate was adjusted to a tilted position of 20°.

2.2.4. Hydrodynamic diameter determination by dynamic light scattering (DLS)

The hydrodynamic diameter determination was performed by measuring the DLS with a Malvern Zetasizer 3000 HSA (Herrenberg, Germany). The particle size analysis of the prepared nanoparticles were performed at 25 °C, an angle of 90° for the photomultiplier and a wavelength of 633 nm. Different analysis types were calculated to verify the DLS results. Auxiliary parameters were: viscosity of the aqueous solutions $cP = 0.891$, refraction index $n = 1.331$. All used liquids were filtered through Millex-GV 0.22 μm Filter Units by Millipore (Molsheim, France).

2.2.5. Surface charge determination of the nanoparticles

The surface charge (zetapotential) of the nanoparticles was determined from the electrophoretic mobility. Measurements were performed using a Malvern Zetasizer HSA 3000 (Herrenberg, Germany). The samples were diluted 1:100 with double distilled water before measuring.

2.2.6. Oligonucleotide loading

To obtain the amount of the oligonucleotides which were bound on the surface of the PBCA-NP preparation, strong anion exchange high performance liquid chromatography (SAX HPLC) was performed. After incubation for 1 h at room temperature the particles with different ratios of ON/NP were centrifuged for 1 h at 100,000 *g*, 25 °C. The supernatants were separated from the pellet. To dissolve the pellets 100 μl of a 20% (w/w) solution of polyphosphate and 400 μl of 1 N sodium hydroxide were added to each sample and the mixture was treated for 1 h in a thermocycler with 1000 rpm at 60 °C. 50 μl of each sample (pellet and supernatant) were injected in the SAX HPLC system, using a Dionex DNApac™ PA-100 (4 × 250 mm) column (Idstein, Germany) and a Merck-Hitachi HPLC system (Darmstadt, Germany), which was equipped with an autosampler L-7200, a gradient pump L-7120, an interface

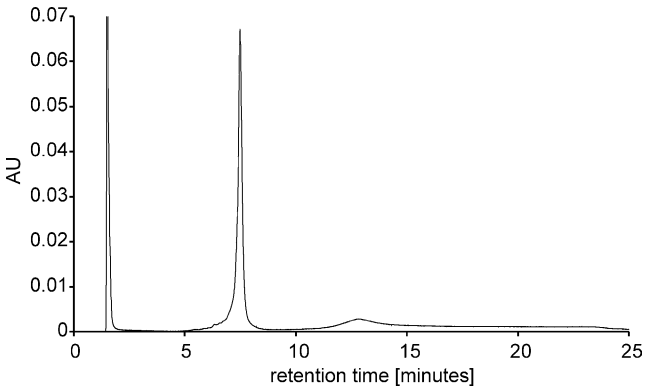

Fig. 1. A typical chromatogram of oligonucleotides determined by SAX HPLC.

D-7000, a diode array detector L-4755, a column oven L-7360 connected to a personal computer system including a HPLC-manager software Version 4.1. The elute solutions consist of (a) 25 mM sodium hydroxide in double distilled water and (b) 25 mM sodium hydroxide, 800 mM sodium perchlorate in double distilled water. The gradient used was 0% (b) for 1 min, 0–100% (b) in 10 min, 10 min 100% (b) linear, 100–0% (b) in 5 min, with a flow rate of 1 ml/min, integrating the signal between 250 and 270 nm. The retention time of the main peak was 7.5 ± 0.02 min and a typical chromatogram is presented in Fig. 1.

2.2.7. Molecular weight determination of PBCA oligochains by matrix assisted laser desorption ionisation-time of flight mass spectrometry (MALDI-TOF MS)

One millilitre of the NP-A preparation including 7 mg of PBCA polymer was dried under vacuum at 25 °C. The residue was dissolved in 1 ml of tetrahydrofuran (THF) afterwards and than mixed with the matrix solution (2,5-dihydroxybenzoic acid in THF 15 mg/ml) in a ratio of 1:5 (v/v). 0.5 μl of this mixture was prepared on a MALDI-TOF MS target and air dried to obtain a fine crystal film. For MALDI-TOF MS a Voyager-DE STR instrument (PerSeptive Biosystems, Framingham, USA) equipped with a N_2-laser ($\lambda = 337$ nm) was used in linear mode. Spectra were accumulated over 1000 shots.

2.2.8. Fluorescence correlation spectroscopy

Fluorescence correlation spectroscopy (FCS) is a powerful technique to determine particle sizes and masses. Furthermore, by labelling different components it is possible to locate different components inside the particles and yield information about the composition of the complexes.

These measurements were carried out with a Zeiss ConfoCor 2 (Jena, Germany). For cross-correlation measurements we utilized a combination of an argon laser (wavelength $\lambda = 488$ nm, excitation of FITC) and HeNe laser ($\lambda = 633$ nm, excitation of Cy™5) to detect molecules or complexes that are tagged with fluorescent dyes of both laser lines. Whereas for single fluophore determination another HeNe laser ($\lambda = 543$ nm, excitation of Rod B) was used.

Measured fluorescence intensity fluctuations can be correlated to the translational diffusion time τ_D (μs) and the average number N of these molecules. The mean residence time of a molecule in the excitation volume is described by the diffusion time. Molecules diffusing into or out of the focal volume induce intensity fluctuations. The normalized autocorrelation function is given by:

$$g(\tau) = 1 + \frac{\langle \Delta I(t)\, \Delta I(t+\tau) \rangle}{\langle I \rangle^2} \tag{1}$$

Here $\Delta I(t)$ displays the average fluorescence intensity fluctuation of molecules at a certain point in time whereas $\Delta I(t+\tau)$ represents the fluctuation at a certain subsequent point in time. $\langle I \rangle^2$ denotes the square of the mean value of the detected intensity. Using two in wavelength different lasers simultaneously in time the normalized crosscorrelation function is given by:

$$g_{br}(\tau) = 1 + \frac{\langle \Delta I_b(t)\, \Delta I_r(t+\tau) \rangle}{\langle I_b \rangle \langle I_r \rangle} \tag{2}$$

The indexes in the term denounce the different channels

$$\frac{\omega_2}{\omega_1} = \mathrm{SP} \tag{3}$$

$$\omega_1 = \sqrt{4D\tau_i} \tag{4}$$

SP indicates the axial structural parameter, calculated from the dimensions of the confocal volume defined by ω_1 (μm) and ω_2 (μm), half of the length of both vertical and horizontal axes of the cylinder (Fig. 2).

SP and ω (μm) were determined by calibration measurements via analysis of aqueous solutions of used fluorescence dyes with calculated values of the diffusion coefficients D (m^2/s). For each fluophore these parameters must be generated individually. Typically, experiments were only run with an SP value within a range of 4–8, which is a main parameter for a proper alignment of this instrument.

To characterise the compounded NP the diffusion coefficient can be calculated out of the measured diffusion

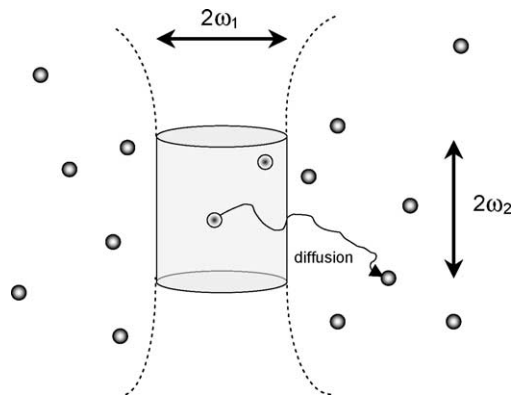

Fig. 2. Schematic illustration of the diffusion of molecules (balls) through the confocal volume which generate fluctuations in the fluorescence signal.

time which can be determined by using an exponential fit (software ConfoCor 2, v.3.2.) of the autocorrelation function. The NP diameter was characterised by the hydrodynamic radius r_h (nm):

$$r_h = \frac{kT}{6\pi\eta D} \quad (5)$$

In this equation, k denotes the Boltzmann constant (1.38×10^{-23} (J/K)), T (K) the absolute temperature and η (g/cm s) indicates the viscosity of the solvent.

The hydrodynamic radius r_h (nm) is related to the molecular weight m [g/mol] of the particles:

$$m = \frac{4\pi r_h^3 N_A \rho}{3} \quad (6)$$

N_A denotes the Avogadro's number (6.023×10^{23} mol^{-1}) and ρ (g/cm^3) the mean density of the molecules or complex.

The calculations were performed with a personal computer system equipped with the Fluorescence Correlation Microscope ConfoCor 2 software, version 3.2 (Carl Zeiss, Jena, Germany).

3. Results and discussion

3.1. Particle characterisation

3.1.1. Preparation methods

Three different preparation methods for cationic PBCA-NP were performed (Fig. 3). Method A forms particles without a fluophore incorporated or attached to the particle (NP-A). Thus these NP could only be investigated by FCS after adsorption of a fluorescence labelled oligonucleotide. To get more information about the formation, size and mass of the PBCA-NP by FCS we developed two methods to label these acrylate nanoparticles with fluorescent dyes. In method B Rhod B-dextran or FITC-dextran was entrapped into the particle matrix (NP-B). In method C the NP were prepared and afterwards derivatized with 5-([4,6-dichlorotriazin-2-yl]amino) fluorescein (DTAF). DTAF reacts with hydroxy groups in basic aqueous solution as shown before [25,26]. Presumably, in our study DTAF was bound to the sugar components or to the PBCA oligomers of the nanoparticles (NP-C) covalently (Fig. 3).

3.2. Particle assembly

3.2.1. FCS measurements

FCS is a well-established technique to determine diffusion coefficient, size and mass of particles, as well as to characterise the binding of low molecular weight ligands to larger receptor molecules in solution. For this application FCS is a well established screening tool in the pharmaceutical industry [27,28]. FCS is a special application of a fluctuation correlation technique, like DLS, where the laser-induced fluorescence of particles out of a very small probe volume (Fig. 2) is autocorrelated to the diffusion-time. A dual-colour instrumental extension of the standard confocal FCS setup enables cross-correlation analysis of two different fluorescent species.

Before polymerisation DEAE-dextran and dextran 70,000 were dissolved in aqueous solution at pH 2.5. In our experiments we have chosen rhodamine B (Rhod B) as fluorescence dye due to the excellent stability of this fluophore during the time resolved measurements covalently bound to

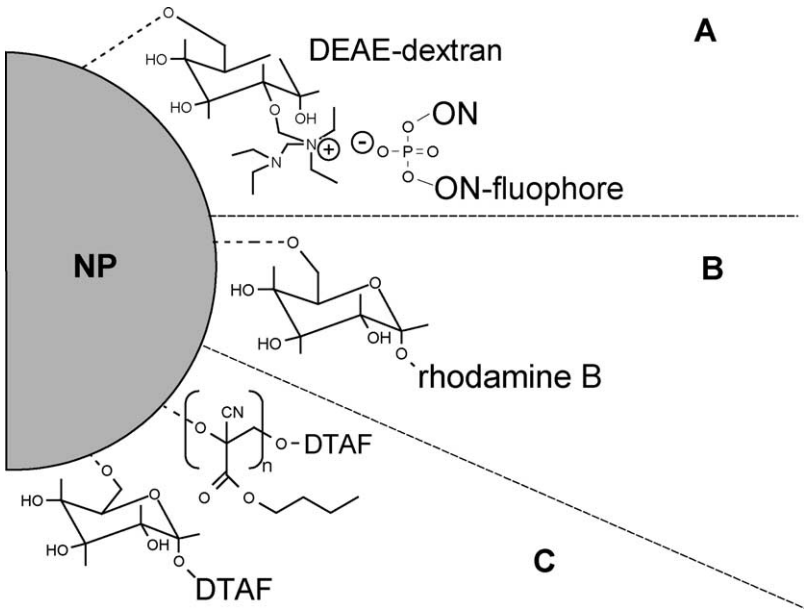

Fig. 3. Schematic chemical structure of the nanoparticle preparation and fluorescence-labelling methods A, B and C.

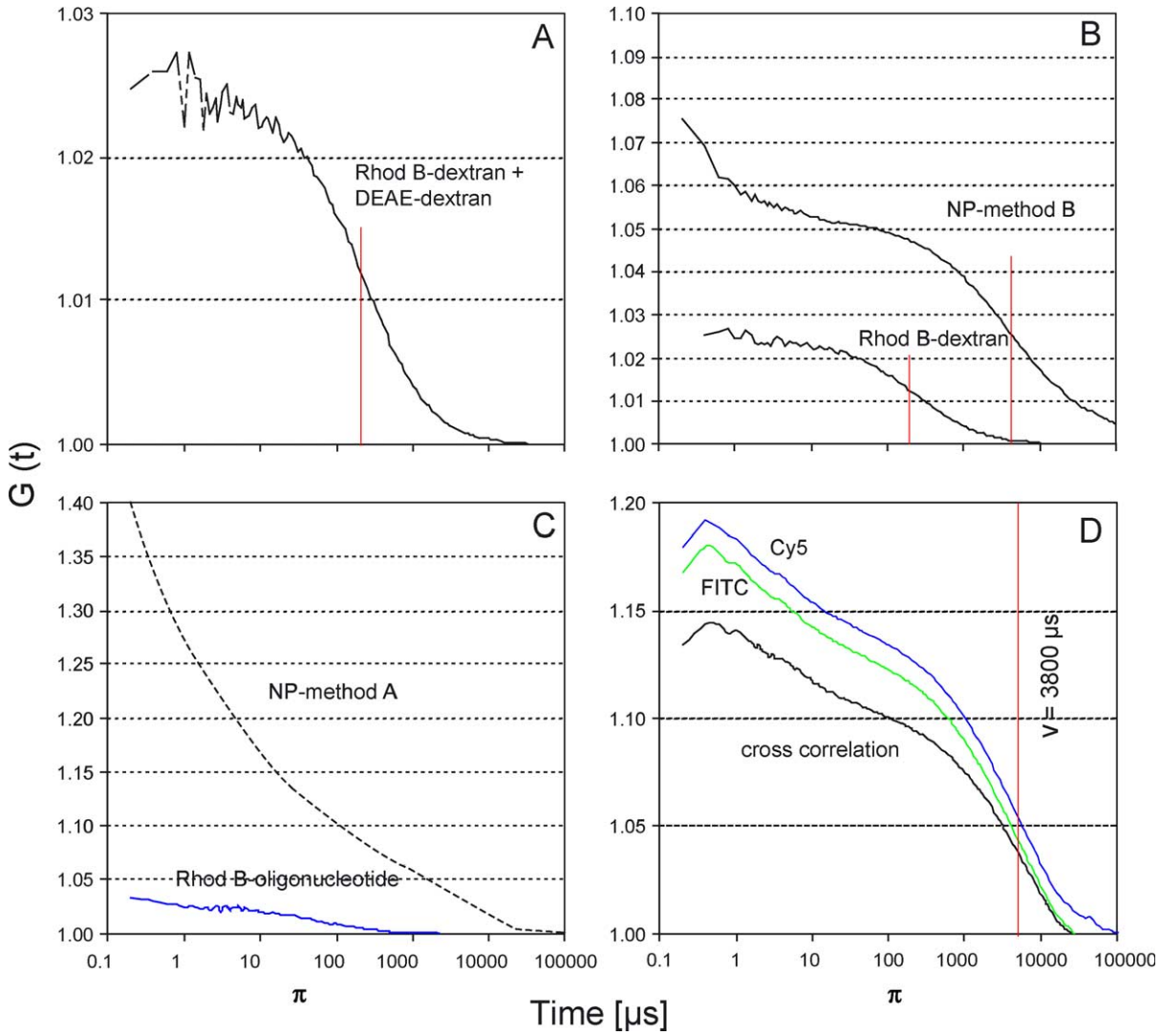

Fig. 4. Correlograms of different FCS measurements. (A) Autocorrelation curve of Rhod B-dextran and DEAE-dextran; (B) autocorrelograms of NP-B and Rhod B-dextran sample; (C) autocorrelograms of NP-A and Rhod B-oligonucleotides; (D) autocorrelograms of NP-B (FITC), Cy5-oligonucleotides and cross-correlation curve of this dual-colour measurement.

dextran 70,000. To characterise the diffusion coefficient [D] of the fluorescent compound in this mixture FCS measurements were employed. As shown in Fig. 4A the diffusion time of the mixture (DEAE-dextran and Rhod B-dextran; pH 2.5) was found to be the same as free Rhod B-dextran (Fig. 4B). From this data we could conclude that DEAE-dextran was adsorbed to dextran 70,000 and no initial starter complex of the different dextrans was observed, otherwise the diffusion time would be shifted to higher values. This result could also be confirmed by DLS measurements. The diffusion coefficient of dextran 70,000 was calculated from the diffusion time which was obtained from the correlation curve (Fig. 4B).

Furthermore, we estimated the average molecular mass of the nanoparticles prepared by method B with a hydrodynamic diameter (d_h) of $d_h = 108$ nm from our FCS measurement (Fig. 4B). Using the information of hydrodynamic radius [r_h] and mean density [ρ] of PBCA in Eq. (6), a molecular weight [m] of approximately 3.6×10^8 Da was calculated for a single NP-B.

3.2.2. Mass spectrometry

To further understand the particle formation and to yield more information about the PBCA polymerisation we performed mass analysis after dissolving NP-A preparation in THF by MALDI-TOF MS technique. Individual fractions of the polymer were detected as $[M\text{-}_n + H_2O + Na]^+$-ions together with their (-30 Da) satellites presumably due to the loss of a terminal hydroxymethylene group. The mass range extends from m/z 806 ($n = 5$) to well above m/z 10,452 ($n = 68$) with an apparent maximum at m/z 1419 ($n = 9$). Within the inspected mass range (m/z 770–10,500) the number average M_n, weight average M_w and polydispersity $D = M_w/M_n$ were calculated as $M_n = 1924$, $M_w = 2253$ and $D = 1.17$ (Fig. 5).

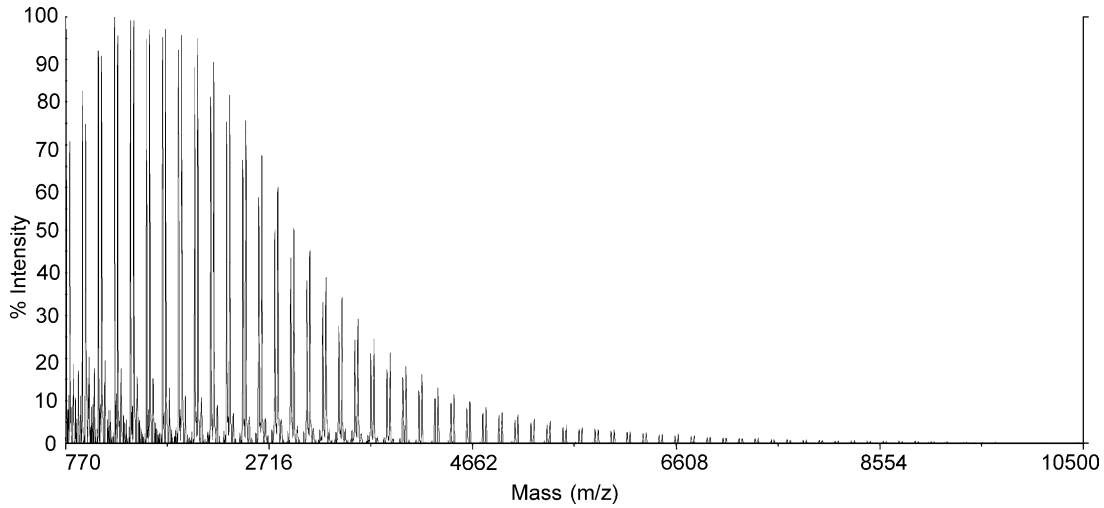

Fig. 5. Analysis of the PBCA oligochain mass distribution in the nanoparticles (NP-A) determined by MALDI-TOF MS.

These findings confirmed that in the first step of particle formation oligomeric chains of PBCA grew in solution until they reached a critical molecular weight [29–31]. After this first polymerisation step the oligomeric chains aggregate in a second step to solid nanoparticles with a much higher molecular weight stabilised by hydrophobic interactions [23,24]. In our MALDI-TOF MS studies we found oligomers with a mass ranging 806–10,452 Da, corresponding to 5–68mer. Performing FCS measurements of nanoparticles preparation (NP-A) an average mass of approximately 3.8×10^8 Da was found for a single nanoparticle. This indicates that the particles are composed of several oligomers. Concluding the findings of both techniques we confirm the theory of the earlier studies which postulated a stepwise nanoparticle formation as described above.

3.2.3. Incorporation of dextran 70,000 and DEAE-dextran

Another interesting question is the incorporation of both sugar components (dextran 70,000 and DEAE-dextran) into the particles. FCS measurements were performed in situ in the colloidal particle suspension (NP-B). In these particles 10% of the dextran 70,000 was exchanged by Rhod B-dextran. By using a two component fit, it was calculated that approximately 89% of the dextran 70,000 was entrapped into the particle matrix (autocorrelation curve is shown in Fig. 4B).

It is interesting that these data are in contradiction to earlier investigations performed by Pirker et al. [32]. In this work was postulated much lower dextran into the particles determined by NMR measurements. One possible explanation for this observation could be that in our recent work in situ measurements were performed in solution whereas the NMR technique was applied only to highly purified samples. Possibly, during particle purification and the washing procedure surface bound dextran was removed which could explain the discrepancy between both investigations.

It could be assumed from the particle formation process discussed earlier that dextrans are located close to the interface between the particle surface and the aqueous medium. This theory was confirmed in our study. Negatively charged oligonucleotides could be adsorbed to positively charged nanoparticles which incorporated the DEAE-dextran. In addition, earlier studies by our group showed that acrylate nanoparticles without DEAE-dextran did not bind ON [14]. By adsorption of a fluorescence labelled ON onto the surface of the NP-A, the diffusion time of the oligonucleotides ($\tau = 66$ μs) was highly prolonged up to about $\tau = 3300$ μs which correlates with the diffusion time of unloaded NP-C. This result indicated that the DEAE-dextran is also entrapped in the particle matrix (Fig. 4C).

3.3. Particle size measurements

3.3.1. FCS and DLS

The size of the NP was calculated by applying different techniques such as DLS, FCS, and the imaging techniques AFM and SEM. The last two techniques were performed to verify the range of the size measurements and to show that the particles are circular in shape, which is an important precondition for the mathematical models for FCS and DLS methods.

With FCS it is possible to calculate the mean hydrodynamic radius (r_h) of the NP directly from the Stoke–Einstein equation (5). Hereby $2r_h$ is the hydrodynamic diameter d_h (nm). Particles which were prepared with method A (NP-A) showed a mean size $d_h = 130 \pm 11$ nm (Table 2) in the FCS measurements. The d_h of the NP-A was determined by adsorbing fluorescence labelled ON (Rhod B-ON) onto the particle surface (Fig. 4C). In addition, the DLS measurements showed a mean size of $d_h = 139 \pm 7$ nm. The polydispersity (PD) of the DLS data were in a range of 0.12–0.15.

Comparing both particle preparations, NP-A and NP-B, it was found that NP-B are significantly smaller than NP-A

Table 2
Mean size of PBCA-NP determined by DLS, SEM, AFM and FCS

Method	Preparation	Diameter (nm)	Fluophore
FCS	A	130 ± 11[a]	Rhod B-ON
DLS	A	139 ± 7[a]	–
SEM	A	140 ± 37[b]	–
AFM	A	122 ± 48[c]	–
FCS	B	108 ± 9[a]	Rhod B
DLS	B	108 ± 12[a]	Rhod B
FCS	C	103 ± 3[a]	DTAF
DLS	C	114 ± 8[a]	DTAF

[a] Representing the arithmetic mean of the mean size (diameter) of three independent samples. The standard deviation was calculated from the mean size of the measurements.
[b] Representing a graphic image analysis of 120 particles (Fig. 6). The standard deviation was calculated from determined diameters.
[c] Representing a graphic image analysis of seven particles (Fig. 7A).

(Student's t-test, $P = 0.048$). A possible reason for this observation could be the lipophilic fluorescence label of the Rhod B-dextran, which could have an influence on the aggregation in the second step of particle formation.

NP which were prepared by method C (NP-C) were also investigated with FCS and DLS. Mean size of $d_h = 103 \pm 3$ nm for FCS and $d_h = 114 \pm 8$ nm for DLS measurements were obtained. These data are in agreement with other fluorescence labelled particles prepared by method B (NP-B).

3.3.2. SEM and AFM

By analysis of the SEM images from NP-A (typical micrograph is shown in Fig. 6) a mean size was calculated as the ferret diameter (d_f) of about 140 ± 37 nm.

To have a closer look on the surface of the NP, AFM measurements were performed. All samples were diluted 10,000 fold to get images of single particles in a high resolution. The particles showed almost a round shape with a smooth surface, which is shown in Fig. 7A and B. A mean size of $d_f = 122 \pm 48$ nm was calculated from the AFM images.

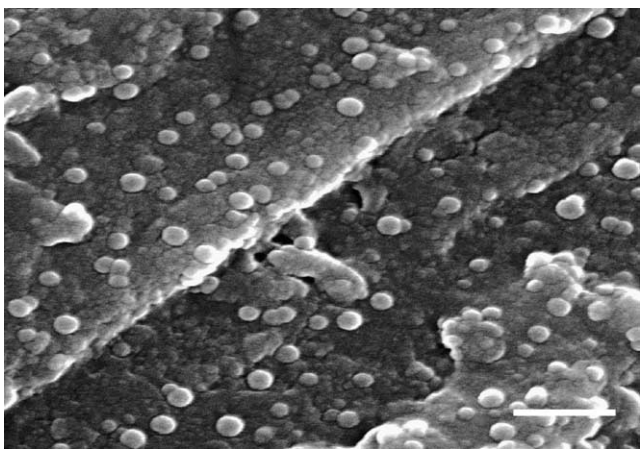

Fig. 6. Scanning electron microscope (SEM) image of nanoparticles (NP-A), scale bar 500 nm.

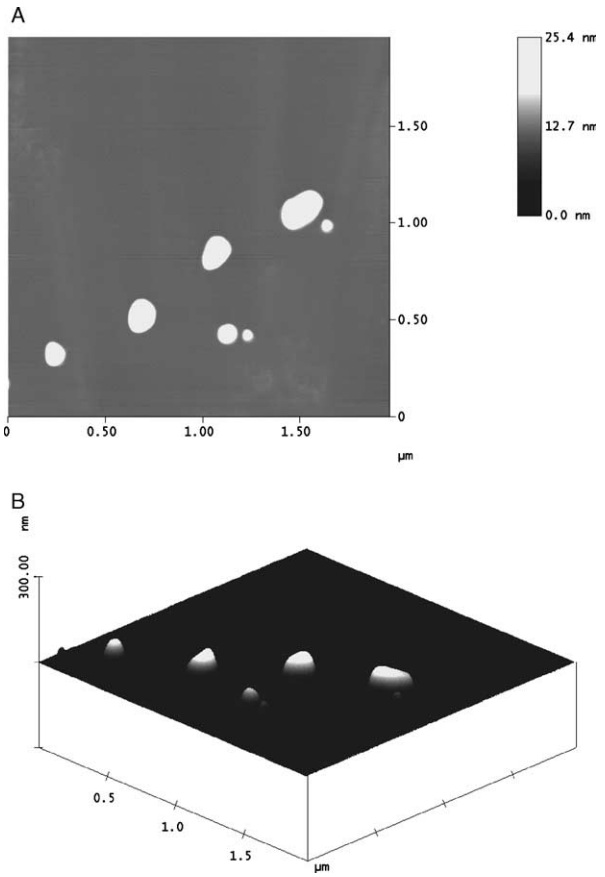

Fig. 7. (A) 2 µm × 2 µm atomic force microscope image of PBCA-NP-A adsorbed and dried on mica. (B) The surface plot of the image of Fig. 6A, displayed as if artificially illuminated from the top.

In conclusion, the mean particle size of NP-A determined from different spectroscopic techniques and imaging methods are in agreement. However, it is interesting that no statistical significant differences (Student's t-test, $P = 0.23$) were found between the hydrodynamic diameter determined from particles in aqueous solution and dried samples from SEM and AFM.

3.4. Characterisation of the interaction between oligonucleotides and nanoparticles

3.4.1. FCS

Polyanions like ON can interact with cationic surfaces by ionic interactions. The kinetics of the adsorption of Rhod B-ON onto the NP-A was determined by FCS measurements with a mass ratio of 1:10 (ON/NP-A). The complexation process was almost finished in less than 20 s which could be verified by fast repeated FCS measurements (sampling period 10 s, six times). Rhod B-ON was adsorbed quantitatively onto the nanoparticles (Fig. 4C) analysed by using a two-component fit where only one component belonging to the Rhod B-ON loaded nanoparticles was

found. The recent data confirm earlier findings from our group and were in correlation with data resulting form MMAE-methacrylate nanoparticle [20].

To verify that the ON were bound to the NP surface, dual-colour fluorescence cross-correlation spectroscopy measurements was carried out [15]. NP-B with an FITC labelled dextran (excitation channel 1, $\lambda = 488$ nm) and ON tagged with a Cy5 fluorescence dye (Cy5-ON) (excitation channel 2, $\lambda = 633$ nm) were used. The configuration of the Zeiss Confocor II allows detection of a complex of two different fluorescence labels in a small confocal volume simultaneously which are spectrally well separated and covalent bound to each component of the ON/NP complex. It was clearly shown that the Cy5-ON was colocalised with the NP-B (Fig. 4D). These data confirm the finding of the single channel FCS measurements.

3.4.2. Zetapotential

Zetapotential measurements were performed to characterise the surface charge of cationic nanoparticles by a charge titration experiment. The information derived from this method are of importance to characterise the loading of oligonucleotides on the nanoparticle surface.

A constant amount of NP-A (100 μg) was incubated with different amounts of ON (12.5–200 μg) in water. Unloaded NP-A showed a positive zetapotential of approximately +39 mV. By increasing the amount of ON in the samples the zetapotential decreased as shown in Fig. 8. For example by adding 100 μg ON to 100 μg NP-A the zetapotential obtained was approximately −40 mV. Beyond this mass of ON absorbed the surface charge only decreased slightly in the mixture. This finding indicated that upon a mass ratio of 1:1 (ON/NP) the total surface of the NP was saturated with ON.

3.4.3. Oligonucleotide loading

The loading of unlabelled ON was characterised in a set of different ON/NP-A ratios, the particles were incubated similarly to the zetapotential measurements. Three different series of measurements were carried out (Fig. 9). At first, between 12.5 and 200 μg of ON were added to 100 μg of NP-A in 1 ml double distilled water and these samples were centrifuged for 1 h in an ultracentrifuge at 100,000 × g. Then the supernatants were separated from the pellet. Afterwards, the pellets were dissolved and the ON which was bound to the NP (Q_p) was quantified by SAX HPLC measurements as described in Section 2.2.6. The amount of ON in the supernatant samples (Q_s) was also determined by this method to ensure the measurements of the pellets (data not shown). The recovery of the ON quantification by SAX HPLC calculated by adding up the Q_p and Q_s in relation to the amount used was larger than 92% for all measurements. As a result, 100 μg of NP-A could be saturated with approximately 20 μg ON. In samples including more than 20 μg ON, unbound oligonucleotides were found in the supernatant samples.

These data could be verified by FCS measurements according to the procedure described before with the supernatant samples to quantify Q_s after centrifugation. Afterwards Q_p was calculated as the difference between the total ON amount and Q_s. This series of measurements showed almost the same Q_p compared to the SAX HPLC findings.

In addition to HPLC technologies with the FCS a new method is available to investigate ON/NP complexes directly in the colloidal solution without separation of unbound ON by centrifugation. In this study, NP-A were loaded with ON at the same ratio described before but without stressing the system by ultracentrifugation. As an important result, a much higher Q_p was obtained in comparison to the samples which were centrifuged.

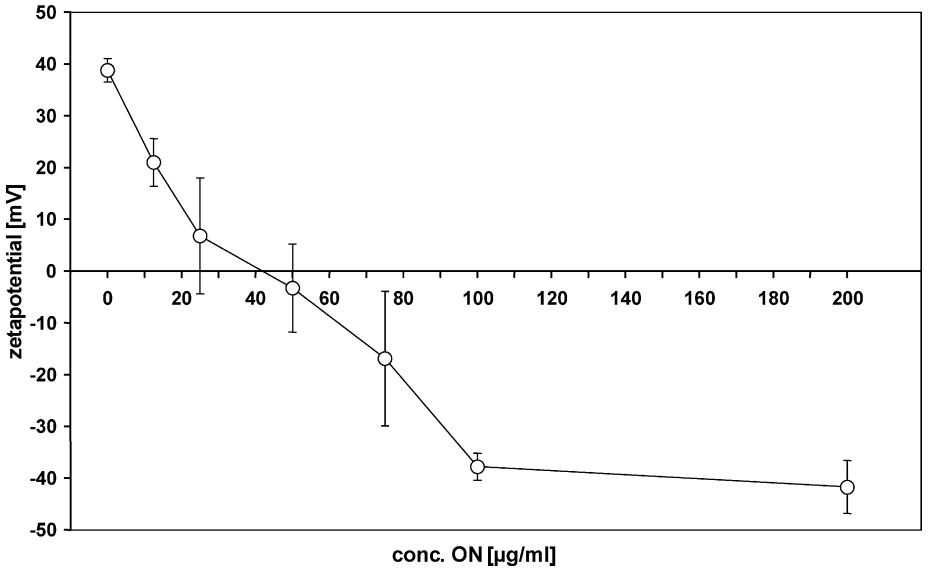

Fig. 8. Surface charge (zetapotential) measurements of nanoparticle (NP-A) incubated with different amount of ON.

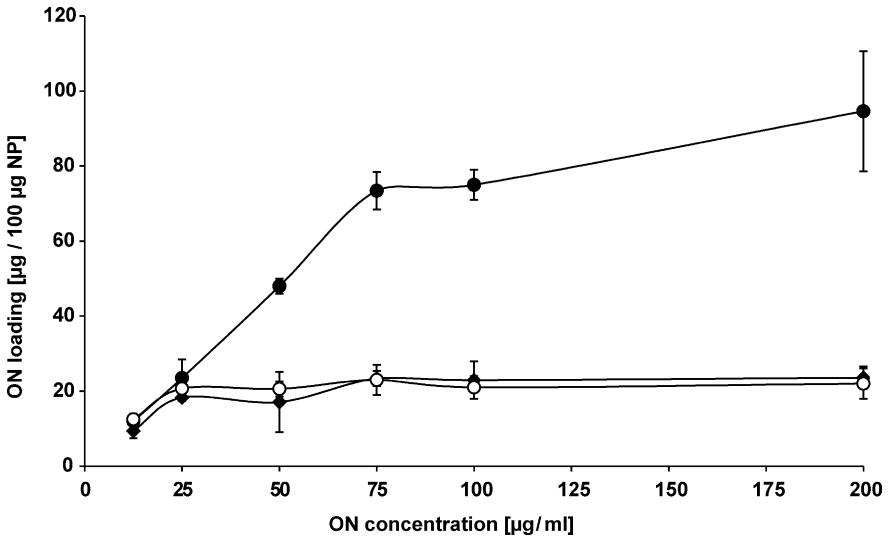

Fig. 9. Determination of the loading rates of NP-A with different concentrations of ON, measured (●) in situ measurements using FCS, (◆) after centrifugation using FCS and (○) after centrifugation using SAX HPLC.

In contradiction to the HPLC measurements, a much larger oligonucleotide loading was observed from in situ FCS measurements, but only at high ON/NP-ratios and at ON concentrations larger than 25 μg/ml (Fig. 9). A possible explanation for this controversial result could be the ultracentrifugation step. With this purification procedure ON could be removed partly from the particle surface as described for dextrans before.

It can be assumed that a static layer of ions is almost fixed directly to the surface of the colloid. Around this layer a mobile layer of ions is located (outer Helmholtz plane) which could be removed by shear stress like centrifugation and pellet formation. Thus, different Q_p rates were found for the unstressed and centrifuged samples.

Further, the results from this paper are consistent with earlier investigations with MMAE-methacrylate nanoparticles. For this type of cationic carrier a correlation between SAX HPLC loading data and FCS measurements was found especially at low oligonucleotide concentrations of approximately 5 μg/ml [20].

4. Conclusion

In summary the FCS technique has been found to be a useful tool for characterisation of colloidal drug delivery systems. Using FCS it was possible to yield information about the amount of the different components in the NP. Determination of mean particle size by FCS matched with a small error to DLS, SEM and AFM techniques. In addition the molecular weight of the NP could be estimated and complexes could be characterised in analytical matrices. For this approach two new methods for fluorescence labelling of cationic particles were developed. This challenge has been achieved by entrapping fluorescence labelled dextran 70,000 into the particle matrix and the derivatisation of hydroxyl groups of the NP by DTAF.

Acknowledgements

This project is supported by Deutsche Forschungsgemeinschaft (DFG) SFB 579, the Graduiertenkolleg GK 137/3 and the Bundesministerium für Bildung und Forschung (BMBF) FKZ 03C0308C, Germany. The authors would like to thank Mr Manfred Ruppel from the Botanic Institute of the Johann Wolfgang Goethe-University, Frankfurt am Main, Germany, for his assistance at the electron microscope, Dr Thomas Russ from the Institute of Pharmaceutical Chemistry of the Johann Wolfgang Goethe-University, Frankfurt am Main, Germany, for his assistance at the mass spectroscope, Mr Alexander Bootzi from the Institute for Pharmaceutical Technology of the Johann Wolfgang Goethe-University, Frankfurt am Main, Germany, Dr Anke Friese and Astrid Weyermann for the helpful discussions. Special thanks are due to Prof. Gernot Tilz, Clinical Immunology at the University of Graz, for his overall support to this project.

References

[1] J. Kreuter, Evaluation of nanoparticles as drug-delivery systems. I: preparation methods, Pharm. Acta Helv. 58 (1983) 196–209.
[2] P. Couvreur, C. Malvy, Pharmaceutical Aspects of Oligonucleotides, vol. 1, Taylor & Francis, London, 2000.
[3] P.C. Zamecnik, M.L. Stephenson, Inhibition of Rous sarcoma virus replication and cell transformation by a specific oligodeoxynucleotide, Proc. Natl. Acad. Sci. USA 75 (1978) 280–284.
[4] M.L. Stephenson, P.C. Zamecnik, Inhibition of Rous sarcoma viral RNA translation by a specific oligodeoxyribonucleotide, Proc. Natl. Acad. Sci. USA 75 (1978) 285–288.

[5] E. Fattal, C. Vauthier, I. Aynie, Y. Nakada, G. Lambert, C. Malvy, P. Couvreur, Biodegradable polyalkylcyanoacrylate nanoparticles for the delivery of oligonucleotides, J. Control. Release 53 (1998) 137–143.
[6] I. Lebedeva, L. Benimetskaya, C.A. Stein, M. Vilenchik, Cellular delivery of antisense oligonucleotides, Eur. J. Pharm. Biopharm. 50 (2000) 101–119.
[7] I. Lebedeva, C.A. Stein, Antisense oligonucleotides: promise and reality, Annu. Rev. Pharmacol. Toxicol. 41 (2001) 403–419.
[8] C. Chavany, T. Le Doan, P. Couvreur, F. Puisieux, C. Helene, Polyalkylcyanoacrylate nanoparticles as polymeric carriers for antisense oligonucleotides, Pharm. Res. 9 (1992) 441–449.
[9] G. Schwab, C. Chavany, I. Duroux, G. Goubin, J. Lebeau, C. Helene, T. Saison-Behmoaras, Antisense oligonucleotides adsorbed to polyalkylcyanoacrylate nanoparticles specifically inhibit mutated Ha-ras-mediated cell proliferation and tumorigenicity in nude mice, Proc. Natl. Acad. Sci. USA 91 (1994) 10460–10464.
[10] H.P. Zobel, M. Junghans, V. Maienschein, D. Werner, M. Gilbert, H. Zimmermann, C. Noe, J. Kreuter, A. Zimmer, Enhanced antisense efficacy of oligonucleotides adsorbed to monomethylaminoethylmethacrylate methylmethacrylate copolymer nanoparticles, Eur. J. Pharm. Biopharm. 49 (2000) 203–210.
[11] H.P. Zobel, A. Zimmer, S. Atmaca-Abdel Aziz, M. Gilbert, D. Werner, C.R. Noe, J. Kreuter, F. Stieneker, Evaluation of aminoalkylmethacrylate nanoparticles as colloidal drug carrier systems. Part I: synthesis of monomers, dependence of the physical properties on the polymerization methods, Eur. J. Pharm. Biopharm. 47 (1999) 203–213.
[12] H.P. Zobel, F. Stieneker, S. Atmaca-Abdel Aziz, M. Gilbert, D. Werner, C.R. Noe, J. Kreuter, A. Zimmer, Evaluation of aminoalkylmethacrylate nanoparticles as colloidal drug carrier systems. Part II: characterization of antisense oligonucleotides loaded copolymer nanoparticles, Eur. J. Pharm. Biopharm. 48 (1999) 1–12.
[13] W.M. Bertling, M. Gareis, V. Paspaleeva, A. Zimmer, J. Kreuter, E. Nurnberg, P. Harrer, Use of liposomes, viral capsids, and nanoparticles as DNA carriers, Biotechnol. Appl. Biochem. 13 (1991) 390–405.
[14] H.P. Zobel, J. Kreuter, D. Werner, C.R. Noe, G. Kumel, A. Zimmer, Cationic polyhexylcyanoacrylate nanoparticles as carriers for antisense oligonucleotides, Antisense Nucleic Acid Drug Dev. 7 (1997) 483–493.
[15] U. Kettling, A. Koltermann, P. Schwille, M. Eigen, Real-time enzyme kinetics monitored by dual-color fluorescence cross-correlation spectroscopy, Proc. Natl. Acad. Sci. USA 95 (1998) 1416–1420.
[16] P. Schwille, Fluorescence correlation spectroscopy and its potential for intracellular applications, Cell Biochem. Biophys. 34 (2001) 383–408.
[17] B.J. Berne, R. Pecora, Dynamic Light Scattering—With Applications to Chemistry, Biology, and Physics, vol. 2, Dover, Mineola, NY, 2000.
[18] R. Pecora, Dynamic light scattering measurement of nanometer particles in liquids, J. Nanoparticle Res. 2 (2000) 123–131.
[19] W.A. Ausserer, M.L. Biros, High-resolution analysis and purification of synthetic oligonucleotides with strong anion-exchange HPLC, Biotechniques 19 (1995) 136–139.
[20] F. Delie, R. Gurny, A. Zimmer, Fluorescence correlation spectroscopy for the characterisation of drug delivery systems, Biol. Chem. 382 (2001) 487–490.
[21] E. Van Rompaey, Y. Chen, J.D. Muller, E. Gratton, E. Van Craenenbroeck, Y. Engelborghs, S. De Smedt, J. Demeester, Fluorescence fluctuation analysis for the study of interactions between oligonucleotides and polycationic polymers, Biol. Chem. 382 (2001) 379–386.
[22] E. Van Rompaey, Y. Engelborghs, N. Sanders, S.C. De Smedt, J. Demeester, Interactions between oligonucleotides and cationic polymers investigated by fluorescence correlation spectroscopy, Pharm. Res. 18 (2001) 928–936.
[23] S.J. Douglas, L. Illum, S.S. Davis, Particle size and size distribution of poly(butyl 2-cyanoacrylate) nanoparticles, J. Colloid Interface Sci. 103 (1985) 154–163.
[24] S.J. Douglas, L. Illum, S.S. Davis, Poly(butyl 2-cyanoacrylate) nanoparticles with different surface charge, J. Control. Release 3 (1986) 15–23.
[25] N.A. Stearns, S. Prigent-Richard, D. Letourneur, J.J. Castellot Jr., Synthesis and characterization of highly sensitive heparin probes for detection of heparin-binding proteins, Anal. Biochem. 247 (1997) 348–356.
[26] D. Letourneur, D. Logeart, T. Avramoglou, J. Jozefonvicz, Antiproliferative capacity of synthetic dextrans on smooth muscle cell growth: the model of derivatized dextrans as heparin-like polymers, J. Biomater. Sci. Polym. Edn 4 (1993) 431–444.
[27] T. Winkler, U. Kettling, A. Koltermann, M. Eigen, Confocal fluorescence coincidence analysis: an approach to ultra high-throughput screening, Proc. Natl. Acad. Sci. USA 96 (1999) 1375–1378.
[28] M.A. Medina, P. Schwille, Fluorescence correlation spectroscopy for the detection and study of single molecules in biology, Bioessays 24 (2002) 758–764.
[29] R. Fitch, The homogeneous nucleation of polymer colloids, Br. Polym. J. 5 (1973) 467–483.
[30] R. Fitch, M. Prenosil, The mechanism of particle formation in polymer hydrosols, J. Polym. Sci. Part C 27 (1969) 95–118.
[31] R. Fitch, C. Tsai, Polymer colloids: particle formation in nonmicellar systems, Polym. Lett. 8 (1970) 703–710.
[32] S. Pirker, J. Kruse, C. Noe, K. Langer, A. Zimmer, J. Kreuter, Characterization of polybutyleyanoacrylate nanoparticles. Part II: determination of polymer content by NMR-analysis, Int. J. Pharm. 128 (1996) 189–195.